*Articles*

# Kinetic Mechanism and Inhibitor Characterization for c-jun-N-Terminal Kinase 3α1

Brian Ember, Ted Kamenecka, and Philip LoGrasso*

*Department of Molecular Therapeutics and Drug Discovery, The Scripps Research Institute, Scripps Florida, 5353 Parkside Drive, Jupiter, Florida 33458*

*Received September 11, 2007; Revised Manuscript Received January 8, 2008*

ABSTRACT: c-jun-N-Terminal kinase 3α1 (JNK3α1) is a mitogen-activated protein (MAP) kinase family member expressed primarily in the brain that phosphorylates protein transcription factors including c-jun and activating transcription factor 2 (ATF2) upon activation by a variety of stress-based stimuli. In this study, the kinetic mechanism for JNK3α1 was determined via initial velocity patterns in the presence and absence of both ATP and ATF2 competitive inhibitors. Peptide inhibitors from both ATF2 (peptide **1**) and JNK-interacting protein 1 (JIP-1) (peptide **3**), derived from the homologous δ-domain JNK docking sequence, inhibited JNK3α1 activity in a competitive fashion versus ATF2 while being pure noncompetitive toward ATP. In contrast, peptides derived from the phosphoacceptor activation domain on ATF2 (peptides **4** and **5**) were recognized neither as substrates nor as inhibitors of JNK3α1. AMP−PCP and compound **6**, a small molecule analinopyrimidine, exhibited pure noncompetitive inhibition versus ATF2 and competitive inhibition versus ATP. Peptide inhibitors based on the δ-domain sites of JIP (**3**) and ATF2 (**1**) were not recognized by p38, also of the MAPK family, which may give insight into finding more selective inhibitors for the JNK family of kinases. Collectively these data showed that JNK3α1 proceeded by a random sequential kinetic mechanism and that the ATP and ATF2 substrate sites were non-interacting. Moreover, these results established the 11-mer JIP peptide (**3**) as a potent ($K_i = 25 \pm 6$ nM) competitive inhibitor versus ATF2 in JNK3α1.

The c-jun $NH_2$-terminal kinases (JNKs)[1] are members of the mitogen-activated protein (MAP) kinase family, a group of serine/threonine kinases receiving interest over the past decade for their direct participation in a variety of cell signaling pathways. Functional MAP kinases are implicated in processes including metabolic reactions, gene regulation and cell proliferation, differentiation, and mobility (*1*). Dysfunction in these pathways has been related to cancer, diabetes, and inflammatory disease (*2*). Specifically, JNKs are activated by environmental stressors including cytokines, high osmolality, UV radiation, and hypoxia (*3, 4*). Upon activation, JNKs phosphorylate c-jun and ATF2, among other transcription factors, which proceed to mediate stimulus-dependent responses (*5–7*).

The JNK subfamily is composed of 3 distinct genes, JNK1, JNK2, and JNK3, which are further spliced into at least 10 isoforms (*6*). Although there is a high sequence homology between the three JNKs (*8*), JNK3 is uniquely expressed primarily in the brain with low levels in the heart and testis, whereas JNKs 1 and 2 are expressed ubiquitously (*9*). Within the brain, JNK3 is further localized into neurons of the hippocampus and layers of the neocortex (*10*). JNKs are activated by phosphorylation of the threonine and tyrosine residues in the activation loop (TXY) observed in all MAP kinases (*6, 8*). Specifically, JNK3 requires phosphorylation by MKK7 to achieve catalytic properties and dual phosphorylation by MKK7 and MKK4 for maximal enzyme activity (*11*). In recent studies, JNK3 knockout mice possessed resistance to excitotoxic pathways including kainic acid induced seizure (*5*) and neuronal apoptosis via 1-methyl-4-phenyl-1,2,3,6-tetrahydropyridine (MPTP), a common tool utilized to mimic Parkinson's disease related damage (*12*). Neuronal cells from JNK3 negative mice also have resistance to Aβ-induced apoptosis, the characteristic lesion of Alzheimer's disease (*13*). Therefore, there has been an increased interest in the gene-specific modulation of JNK3 as a therapeutic target for a variety of neurodegenerative diseases.

Approximately 520 genes in the human kinome signify the vast biological relevance of phosphorylation events (*14*). As ATP serves as the phosphate donor for this vast number of kinases, selectivity and specificity for individual kinases

* Author to whom correspondence should be addressed [telephone (561) 799-8881; fax (561) 799-8959; e-mail lograsso@scripps.edu].

[1] Abbreviations: JNK, c-jun $NH_2$-terminal kinases; MAP(K), mitogen-activated protein (kinase); ATF2, activating transcription factor 2; MKK, MAP kinase kinase; MPTP, 1-methyl-4-phenyl-1,2,3,6-tetrahydropyridine; ATP, adenosine triphosphate; AMP-PCP, β,γ-methyleneadenosine 5′-triphosphate; GSK3, glycogen synthase kinase 3; PDK1, phosphoinositide-dependent protein kinase-1; ERK2, extracellular signal-regulated protein kinase 2; JIP, JNK-interacting protein; cAPK, cAMP-dependent protein kinase; IPTG, isopropylthio-β-galactoside; EDTA, ethylenediaminetetraacetic acid; HEPES, *N*-(2-hydroxyethyl)-piperazine-*N*′-2-ethanesulfonic acid; DTT, dithiothreitol; BSA, bovine serum albumin; GST, glutathione *S*-transferase; EGRF, epidermal growth factor receptor; MEK, MAP-ERK kinase; MK2, MAPKAP2, mitogen-activated protein kinase-activated protein 2.

10.1021/bi701852z CCC: $40.75 
Published on Web 02/13/2008

may be located in the less conserved substrate domains. Recently, a number of serine/threonine kinase members including the MAPK, glycogen synthase kinase 3 (GSK3), and phosphoinositide-dependent protein kinase-1 (PDK1) families have been found to utilize direct docking interactions with substrates at sites distinct from the phosphorylation site (*15*). These distinct δ-domains are conventionally located fewer than 100 amino acids N-terminal to the activation domain, although certain ETS transcription factors possess an ERK2 δ-site C-terminal to the phosphoacceptor sequence (*16*). These docking motifs have been found in nuclear and cytoplasmic substrates as well as in activators and repressors of MAPK activity (*17, 18*). More specifically, JNK δ-sites of c-jun and ATF2 have been identified with a deletion of these domains preventing phosphorylation (*19, 20*). Although certain δ-domains are recognized by multiple MAPKs, an additional role of these domains is to enhance specificity (*21*). Additionally, the δ-domains are reported to determine phosphorylation sites within the substrates. As c-jun is normally bis-phosphorylated on serines 63 and 73, deletion of the δ-domain produces a switch to alternative phosphorylation sites (*22*). Finally, the δ-sites of scaffold proteins such as JNK-interacting proteins (JIPs) bind to MAP kinases to form complexes that modulate signal transduction cascades (*23–25*).

Understanding the detailed kinetic mechanism of enzyme catalysis conveys information necessary for the development of potent inhibitors. Enzymes catalyzing a two-substrate reaction, including all kinases, can display either a sequential pattern in which both substrates associate with the enzyme prior to catalysis forming a ternary complex or a ping-pong mechanism in which one substrate is bound, chemical transformation occurs, and product is dissociated prior to the association of the second substrate. For sequential mechanisms, the binding of substrates may be ordered or random in nature. Beginning in 1982 with the discovery of the kinetic mechanism for cAMP-dependent protein kinase (cAPK) by Cook et al., mechanistic studies of serine/threonine kinases have been prominently reported throughout the literature (*26*). Cook et al. reported that cAPK proceeded by a random sequential mechanism, which was contradicted by the findings of Whitehouse et al., who indicated an ordered pattern with ATP binding first (*27, 28*). Steady-state data for the MAP kinase p38 support an ordered sequential mechanism with ATF2 binding first (*29*). Recently, the mechanism for JNK2 was reported as a random sequential mechanism with ATF2 and ATP (*30*).

The current study was designed to investigate the kinetic mechanism for JNK3α1 and to compare competitive inhibition of the ATP pocket, the ATF2 pocket, and the distal δ-domain docking groove. Steady-state kinetic analysis of the incorporation of a $^{33}$P-labeled phosphate from γ-$^{33}$P ATP into biotinylated-FLAG-ATF2 (b-FL-ATF2) was utilized to determine catalytic efficiency and inhibitor binding mechanisms. The ATP analogue AMP−PCP and compound **6** were employed as ATP competitive inhibitors and peptides of the JIP-1 (**3**) and ATF2 (**1**) δ-docking site as ATF2 competitive inhibitors. Furthermore, different length ATF2 peptides as well as those containing the phosphoacceptor activation domain but not the δ-domain docking sequence revealed more in-depth recognition analysis of JNK3α1 and specificity versus p38. The study demonstrates that JNK3α1 kinase proceeded via a random sequential kinetic mechanism. Additionally, although the shorter ATF2 peptide docking sequence (**2**) is required for recognition, increasing the length of the sequence (**1**) greatly increased the affinity of the enzyme−peptide complex.

## MATERIALS AND METHODS

*Expression and Purification of Proteins.* Expression and purification of JNK3α1 (amino acids 39–422) followed the protocol of Lisnock et al. (*11*). JNK2α2 and JNK1α1 were purchased from Millipore. Biotinylated-Flag-ATF2 (b-FL-ATF2) was expressed in *Escherichia coli* strain BL21 DE3star (Invitrogen) under the following conditions: 2 mL of a log phase culture grown in Miller's Luria broth (LB) (Cellgro) supplemented with 100 μg/mL ampicillin (Sigma) and 34 μg/mL chloramphenicol (Sigma) was transferred to 1 L of the same medium with shaking at 210 rpm and 37 °C. At $A_{600}$ = 0.6, 0.05 mM d-biotin (Supelco) was added to biotinylate the bioease tag followed immediately by induction with 0.5 mM (final concentration) isopropylthio-β-galactoside (IPTG) (Gibco) and grown with shaking at 210 rpm and 37 °C for 2 h and harvested at 4 °C by centrifugation at 4000*g*. Cell pellets were frozen at −70 °C for subsequent purification.

Frozen pellets from a 1 L culture were resuspended in 10 mL of B-per lysis buffer (Pierce) with complete Mini EDTA-free protease Inhibitor Cocktail (Roche). Cells were lysed by the addition of lysozyme chloride grade VI from chicken egg white and deoxyribonuclease I from bovine pancreas (Sigma) followed by sonication (20 s at 10 W with 2 min intervals in ice; three times). The lysate was centrifuged at 20000 rpm for 30 min at 4 °C to provide the supernatant. The supernatant was applied to an Anti-FLAG M2-Agarose column (Sigma), preincubated with a wash buffer (50 mM HEPES, 150 mM NaCl, pH 7.0), followed by 5 column volumes of wash buffer. The protein was eluted with glycine buffer (100 mM glycine, pH 3.5) in 1 mL fractions into Eppendorfs containing 100 μL of 1 M HEPES, pH 8.0. The collected fractions were concentrated using Amicon Ultra-4 (Millipore). SimplyBlue (Invitrogen) staining of 4–12% gradient NuPage Bis-Tris gels (Invitrogen) revealed >95% homogeneity. The concentration of b-FL-ATF2 was determined by BCA protein assay (Pierce).

*Steady-State Kinetics.* Initial velocity studies utilized to determine the steady-state constants for ATP and b-FL-ATF2 were carried out in 50 μL volumes containing the final concentrations of the following: 25 mM HEPES (Sigma), pH 7.4, 10 mM $MgCl_2$ (Sigma); 2 mM DTT (Sigma); 1 mg/mL BSA; 3 μCi [γ-$^{33}$P]ATP (3000 Ci/mmol; 1 Ci = 37 GBq) (Perkin-Elmer) for all reactions except for compound **6** versus b-FL-ATF2, in which 9 μCi was used; 0.25–16 μM ATP (Sigma); and 0.125–8 μM b-FL-ATF2. The reactions were initiated with 2 nM JNK3α1 (final concentration) and incubated for 1 h at 30 °C. Under these conditions, <10% of substrate was converted to product, and the reaction was linear over a time course of up to 2 h. Reactions were quenched with 50 μL of a 100 mM EDTA−15 mM sodium pyrophosphate solution. Twenty microliters of the stopped reaction was spotted in duplicate onto a p81 phosphocellulose circle (Fisher). The samples were allowed to dry before being washed three times with 75 mM phosphoric acid for 3 min

each to remove unincorporated [$\gamma$-$^{33}$P]ATP. A fourth wash of ethanol for 30 s reduced the drying time necessary before addition to 3 mL of ScintiSafe Econo 2 scintillation cocktail (VWR) and counting on a scintillation counter. Data are the average of two experiments spotted in duplicate. The initial velocities as a function of ATP and b-FL-ATF2 were fitted to equations for ternary complex, ternary complex with non-interacting substrate sites, and ping-pong mechanisms (*31*). Kinetic constants were determined from a robust nonlinear least-squares analysis (*31*).

*Enzyme Inhibition.* Enzyme inhibition studies were performed as described for steady-state kinetics. When ATP was the varied substrate, [b-FL-ATF2] was fixed at 0.5 $\mu$M, and when b-FL-ATF2 was the varied substrate, [ATP] was fixed at 2 $\mu$M for ATF2 competitive inhibitors and at 8 $\mu$M for ATP competitive inhibitors. For inhibition experiments, the concentration of AMP−PCP (Sigma) ranged from 100 to 10 $\mu$M; ATF2 $\delta$-site peptide (**1**) (Peptidogenic) ranged from 200 to 6.25 $\mu$M; JIP-1 $\delta$-site peptide (**3**) (Peptidogenic) ranged from 400 to 25 nM; and compound **6** ranged from 2 $\mu$M to 125 nM. The initial velocities were fitted to equations for competitive, uncompetitive, pure noncompetitive, and mixed noncompetitive inhibition, and steady-state rate constants were determined from a robust nonlinear squares fit (*31*). Reactions were spotted in duplicate, and inhibition reactions were performed in duplicate for all inhibitors versus both ATP and b-FL-ATF2. Methods and data for the $IC_{50}$ of JIP (**1**) with JNK1$\alpha$1, JNK2$\alpha$2, and JNK3$\alpha$1 can be found in the Supporting Information.

*Kinetic Analysis.* The kinetic analysis was performed using GraFit version 5 (*31*) fitted to the following equations.

For two-substrate kinetics, ternary mechanism (eq 1), ternary mechanism with non-interacting substrate sites (eq 2), and ping-pong mechanism (eq 3) apply.

$$v = V_{max}[A][B]/(K_{ia}K_{mB} + K_{mB}[A] + K_{mA}[B] + [A][B]) \quad (1)$$

$$v = V_{max}[A][B]/(K_{mA}K_{mB} + K_{mB}[A] + K_{mA}[B] + [A][B]) \quad (2)$$

$$v = V_{max}[A][B]/(K_{mB}[A] + K_{mA}[B] + [A][B]) \quad (3)$$

$V_{max}$ is the maximum initial velocity, A and B represent the substrates, $K_{ia}$ is the dissociation constant for substrate A from free enzyme, and $K_{mA}$ and $K_{mB}$ are the corresponding Michaelis−Mentin constants for A and B.

Inhibition experiments were fitted to competitive (eq 4), pure noncompetitive (eq 5), mixed noncompetitive (eq 6), and uncompetitive (eq 7) models.

$$v = V_{max}[S]/(K_m(1 + [I]/K_{is}) + [S]) \quad (4)$$

$$v = V_{max}[S]/(K_m(1 + [I]/K_i) + [S](1 + [I]/K_i) \quad (5)$$

$$v = V_{max}[S]/(K_m(1 + [I]/K_{is}) + [S](1 + [I]/K_{ii}) \quad (6)$$

$$v = V_{max}[S]/(K_m + [S](1 + [I]/K_{ii})) \quad (7)$$

where S is the varied substrate to which $K_m$ refers, I is the inhibitor, $K_{is}$ is the inhibition constant at varied substrate concentrations $\ll K_m$, derived from the slope of the Lineweaver–Burk plots, and $K_{ii}$ is the inhibition constant at varied substrate concentrations $\gg K_m$, derived from the *y*-intercept of the Lineweaver–Burk plots. For noncompetitive inhibitors, if $K_{is}$ and $K_{ii}$ are equal, eq 6 simplifies to eq 5, giving pure noncompetitive inhibition with the enzyme recognizing the inhibitor equally regardless of substrate concentration. If $K_{is}$ and $K_{ii}$ are not equal, there is mixed noncompetitive inhibition with the enzyme–inhibitor binding dependent upon substrate concentration.

*Synthesis of Compound **6**.* A mixture of 2,4-dichloropyrimidine (5.0 g, 34 mmol), phenylboronic acid (4.5 g, 37 mmol), $Pd(PPh_3)_4$(1.9 g, 1.6 mmol), $K_2CO_3$ (50 mL, 2 M aqueous solution), and DME (55 mL) was placed in a round-bottom flask and heated to 95 °C overnight under argon. The reaction mixture was cooled to room temperature and transferred to a separatory funnel. The layers were separated and the aqueous layer was extracted with ethyl acetate (two times). The combined organics were dried ($MgSO_4$) and concentrated to give 2-chloro-4-phenylpyrimidine.

A mixture of 2-chloro-4-phenylpyrimidine (300 mg, 1.06 mmol) and 4-aminobenzamide (550 mg, 4.04 mmol) in ethoxyethanol (3 mL) and water (1.5 mL) was place in a sealed tube and heated to 120 °C overnight. The reaction mixture was cooled to room temperature, and water was added (5 mL). The resulting precipitate was filtered, washed with water and toluene, and dried under vacuum to give 4-(4-phenylpyrimidin-2-ylamino)benzamide (*32*) as a pale yellow solid, which was judged to be >96% pure by analytical HPLC analysis: $^1$H NMR (DMSO-$d_6$, 400 MHz) $\delta$ 9.9 (s, 1H), 8.6 (d, 1H), 8.20 (br s, 2H), 8.1–7.7 (m, 5H), 7.6 (br s, 3H), 7.5 (d, 1H), 7.15 (br s, 1H); MS (ESI) 291.1 (M + H).

## RESULTS

*Initial Velocity Studies.* The two-substrate profile for JNK3$\alpha$1 MAP kinase was determined by utilizing a two-dimensional matrix of various concentrations of ATP and b-FL-ATF2. Analysis of the double-reciprocal Lineweaver–Burk plots of $1/v$ versus 1/[ATP] and $1/v$ versus 1/[b-FL-ATF2] revealed a pattern of lines converging at an intersection left of the *y*-axis (Figure 1), indicating a sequential kinetic mechanism (*33*). In contrast, a ping-pong mechanism would generate parallel lines from the Lineweaver–Burk plots. The steady-state rate constants from two experiments analyzed in duplicate and generated utilizing eq 2 for a ternary complex with non-interacting substrate sites are summarized in Table 1. The results correlated well with those reported by Lisnock et al. for JNK3$\alpha$1 (*11*). Moreover, the equilibrium dissociation constants generated by eq 1 for a ternary complex ($K_{ia}$) for ATP and b-FL-ATF2 were nearly identical to the corresponding $K_m$ value for each of these substrates (Supporting Information Table S1), indicating non-interacting substrate binding. The lack of interaction between the two substrate sites suggested a random sequential mechanism as opposed to a required order of substrate binding.

*Inhibition of JNK3 by Dead-End Inhibitor AMP-PCP.* To confirm the two-substrate kinetic data suggesting a random ternary mechanism for JNK3, we utilized the dead-end inhibitor AMP-PCP (a nonhydrolyzable ATP analogue) to determine order of substrate binding. Inhibition constants and mode of inhibition for AMP-PCP versus ATP and b-FL-ATF2 are summarized in Table 2. Comparison of the standard error and regression analysis of fits for competitive, pure noncompetitive, mixed noncompetitive, and uncom-

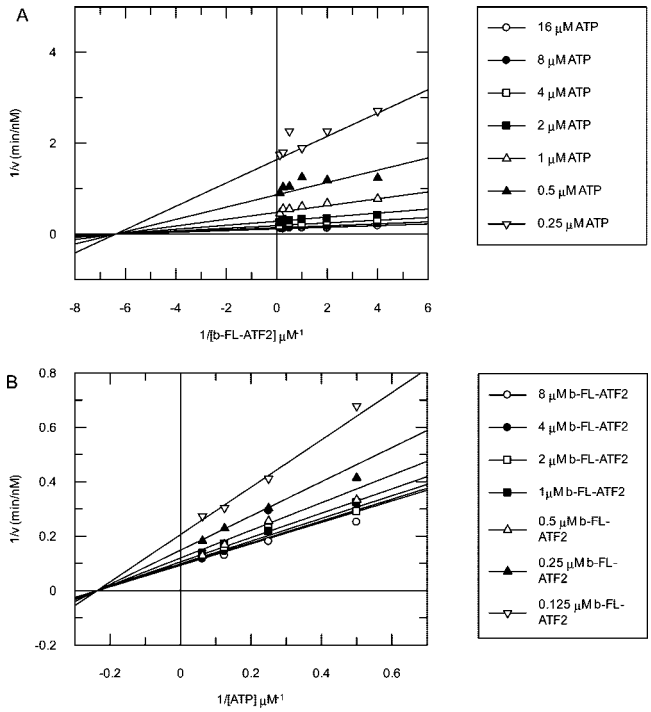


FIGURE 1: Two-substrate profile for JNK3α1 catalyzed b-FL-ATF2 phosphorylation: (A) double-reciprocal plot of $1/v$ (min/nM) versus 1/[b-FL-ATF2] ($\mu M^{-1}$) at seven fixed ATP concentrations; (B) double-reciprocal plot of $1/v$ (min/nM) versus 1/[ATP] ($\mu M^{-1}$) at seven fixed b-FL-ATF2 concentrations. The equation for a ternary complex formation was fit to the experimental data (*31*).

Table 1: Kinetic Constants for JNK3α1 MAP Kinase from Two-Substrate Kinetics[a]

| substrate | $K_m$ ($\mu$M) | $k_{cat}$ ($min^{-1}$) |
|---|---|---|
| b-FL-ATF2 | $0.16 \pm 0.01$ | $5.5 \pm 0.2$ |
| ATP | $4.2 \pm 0.2$ | |

[a] The kinetic parameters were calculated from the equation for a ternary complex with non-interacting sites (eq 2) (*31*). The errors shown are standard errors. Data are from a single experiment performed in duplicate. Repeat experiments yielded identical results.

Table 2: Inhibition Constants and Mode of Inhibition for JNK3α1 MAP Kinase[a]

| inhibitor | varied substrate | inhibition pattern | $K_i$ ($\mu$M) |
|---|---|---|---|
| AMP-PCP | ATP | competitive | $15.5 \pm 0.2$ |
| AMP-PCP | b-FL-ATF2 | pure noncompetitive | $46.5 \pm 1.2$ |
| compound **6** | ATP | competitive | $0.13 \pm 0.01$ |
| compound **6** | b-FL-ATF2 | pure noncompetitive | $1.18 \pm 0.09$ |
| ATF2 δ-domain (long) (**1**) | ATP | pure noncompetitive | $35.6 \pm 1.9$ |
| ATF2 δ-domain (long) (**1**) | b-FL-ATF2 | competitive | $7.1 \pm 1.0$ |
| JIP-1 (**3**) | ATP | mixed noncompetitive | $0.079 \pm 0.012$[b]<br>$0.20 \pm 0.02$[c] |
| JIP-1 (**3**) | b-FL-ATF2 | competitive | $0.025 \pm 0.006$ |

[a] Inhibition constants were calculated from the equation for either competitive, pure noncompetitive, or mixed noncompetitive inhibition (*31*). For mixed noncompetitive data: [b] $K_{is}$ value; [c] $K_{ii}$ value. The errors shown are standard errors. Data are from a single experiment performed in duplicate. Repeat experiments yielded identical results.

petitive inhibition (eqs 4−7) supported competitive inhibition for AMP-PCP versus ATP and pure noncompetitive inhibition versus b-FL-ATF2. Inspection of the Lineweaver–Burk plots (Figure 2) corroborated the calculations as the convergent lines intersected at the *y*-axis (Figure 2A) with varying

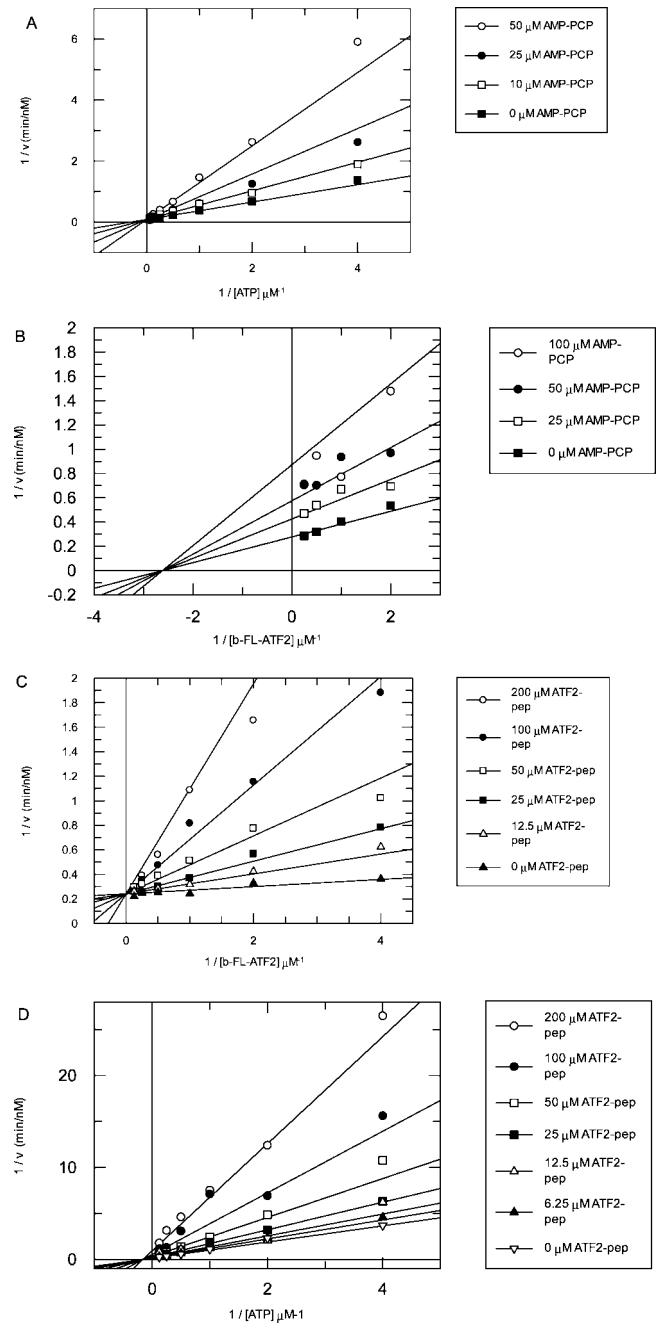


FIGURE 2: AMP-PCP inhibition of JNK3α1: (A) double-reciprocal plot of $1/v$ (min/nM) versus 1/[ATP] ($\mu M^{-1}$) at four fixed AMP-PCP concentrations [the b-FL-ATF2 concentration was fixed at 0.5 $\mu$M; the equation for competitive inhibition was fit to the experimental data (*31*)]; (B) double-reciprocal plot of $1/v$ (min/nM) versus 1/[b-FL-ATF2] ($\mu M^{-1}$) at four fixed AMP-PCP concentrations [the ATP concentration was fixed at 8 $\mu$M; the equation for pure noncompetitive inhibition was fit to the experimental data (*31*)]; (C) double-reciprocal plot of $1/v$ (min/nM) versus 1/[b-FL-ATF2] ($\mu M^{-1}$) at six fixed ATF2-pep (long) (**1**) concentrations [the ATP concentration was fixed at 2 $\mu$M; the data were fit to the equation for competitive inhibition (*31*)]; (D) double-reciprocal plot of $1/v$ (min/nM) versus 1/[ATP] ($\mu M^{-1}$) at seven fixed ATF2-pep (long) (**1**) concentrations [the b-FL-ATF2 concentration was fixed at 0.5 $\mu$M; the equation for pure noncompetitive inhibition was fit to the experimental data (*31*)].

ATP (competitive) and to the left of the *y*-axis (noncompetitive) with varying b-FL-ATF2 (Figure 2B). This mode of inhibition was consistent with the random sequential mech-

Table 3: Peptides and Compound Utilized for Inhibition Studies of JNK3α1 MAP Kinase[a]

| peptide/compound | amino acid sequence | sequence location |
|---|---|---|
| (**1**) ATF2 δ-domain (long) | AVH*K*H*K*HE*M*T*L*KFGPAR | 43-59 |
| (**2**) ATF2 δ-domain (short) | E*M*T*L*KFGPAR | 50-59 |
| (**3**) JIP-1 | *RPKR*PTTLNLF | 153-163 |
| (**4**) ATF2 activation site | VIVADQTPTPTRFLK | 63-77 |
| (**5**) ATF2 activation site mutant | VIVADQAPAPTRFLK | 63-77 |
| (**6**) compound **6** | 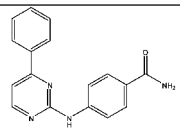 | |

[a] Residues in italic are consensus basic or hydrophobic. Residues in bold are mutations.

anism and with non-interacting substrate binding sites established by our initial velocity studies.

*Inhibition of JNK3 by the δ-Site Binding Peptide of ATF2.* To extend the mechanistic findings from the two substrate and AMP−PCP inhibition data, we investigated the mechanism of inhibition for JNK3 utilizing the δ-site binding peptide of ATF2. The sequence for this peptide is given in Table 3 as peptide **1** and named the ATF2 δ-domain (long). The double-reciprocal plots for this peptide versus b-FL-ATF2 and ATP are given in panels C and D, respectively, of Figure 2, and the inhibition constants and mode of inhibition are presented in Table 2. These results further corroborated a random sequential mechanism. Interestingly, a shorter version of peptide **1**, consisting of only 10 amino acids (peptide **2**), had relatively weak binding affinity to JNK3α1, showing an $IC_{50}$ of approximately 300 μM (Supporting Information Figure S1). Titration of peptide **1** up to 1 mM showed no inhibition of p38, the most closely related MAP kinase to JNK.

*Studies with Other Peptides.* Table 3 summarizes other peptides and one small molecule inhibitor utilized to study MAP kinase protein recognition, inhibition, and selectivity. The ATF2 phosphoacceptor site peptide **4** (containing Thr 69 and Thr 71) was utilized as both a potential substrate and an inhibitor. Peptide **4** was not recognized as a substrate or inhibitor of JNK3 even up to 1 mM. When the two Thr phosphorylation sites of ATF2 were changed to Ala (shown in bold in peptide **5**), no inhibition up to 1 mM was observed. The kinetic analysis of a δ-site peptide of the JIP scaffolding protein (peptide **3**) is summarized in Table 2. JIP peptide (**3**) inhibited JNK3 in a competitive mechanism versus b-FL-ATF2 and in a mixed noncompetitive mechanism versus ATP (Figure 3). JIP peptide (**3**) also showed negligible inhibition of p38 (data not shown). The noncompetitive modes of inhibition versus b-FL-ATF2 for the conserved δ-site peptides **1** and **3**, and specifically the lack of uncompetitive inhibition in which the inhibitor preferentially binds to the enzyme–substrate complex and is visualized by parallel lines in the Lineweaver–Burk plots, again corroborated the random sequential mechanism for JNK3. We also measured the mode of inhibition of JIP peptide (**3**) versus JNK2α2. JIP peptide (**3**) inhibited JNK2α2 with the same mode of inhibition and inhibition constants similar to that of JNK3 (Supporting Information Table S2). To investigate whether there were any differences between the inhibition of JIP peptide (**3**) versus JNK1α1, JNK2α2, and JNK3α1, we determined the $IC_{50}$ values (Supporting Information Table S3 and Figure S1, B−D).

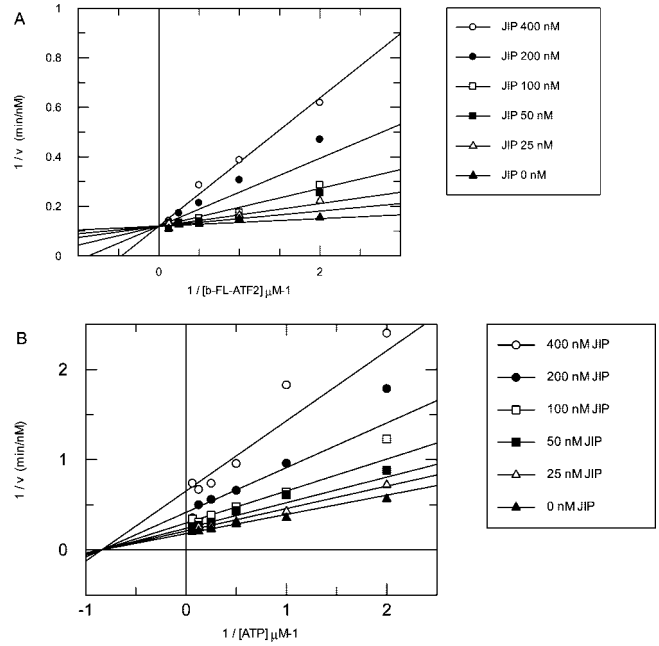


FIGURE 3: JIP peptide inhibition of JNK3α1: (A) double-reciprocal plot of $1/v$ (min/nM) versus 1/[b-FL-ATF2] ($\mu M^{-1}$) at six fixed JIP concentrations [the ATP concentration was fixed at 2 μM; the equation for competitive inhibition was fit to the experimental data (*31*)]; (B) double-reciprocal plot of $1/v$ (min/nM) versus 1/[ATP] ($\mu M^{-1}$) at six fixed JIP concentrations [the b-FL-ATF2 concentration was fixed at 0.5 μM; the equation for mixed noncompetitive inhibition was fit to the experimental data (*31*)].

*Inhibition by Compound **6**.* An anilinopyrimidine derivative inhibitor of JNK3 (Table 2) was analyzed to determine the mechanism of inhibition. Standard error and regression analysis and inspection of the Lineweaver–Burk plots demonstrated that compound **6** is a competitive inhibitor versus ATP (Figure 4A) and a pure noncompetitive inhibitor versus b-FL-ATF2 (Figure 4B). The inhibition constants and mode of inhibition are given in Table 2.

## DISCUSSION

*Kinetic Mechanism.* In our study, we determined the kinetic mechanism for the Ser/Thr kinase JNK3α1 of the MAPK family. Mechanistic studies on Ser/Thr kinases beginning with cAPK (*26–28*) and continuing with other MAPK family members including p38 (*29, 34*) and JNK2 (*30*) have emphasized the importance in determining the kinetic mechanism of these enzymes. Recent focus on targeting JNK3 in neurodegenerative diseases makes a thorough understanding of this enzyme critical.

Utilizing a combination of initial velocity studies and dead-end inhibition analysis, we have generated a collection of data that indicated a random sequential kinetic mechanism requiring a ternary complex of JNK3, ATP, and b-FL-ATF2. The two-substrate profile for JNK3 with ATP and b-FL-ATF2 excluded a ping-pong mechanism due to the intersecting line pattern observed in the double-reciprocal plot (*35*). The initial velocity data also showed no disparity between

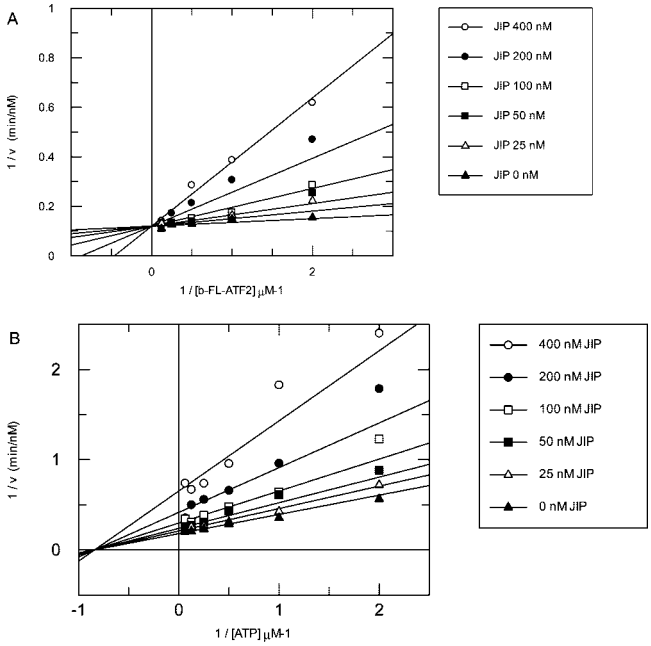


FIGURE 4: Compound **6** inhibition of JNK3α1: (A) double-reciprocal plot of $1/v$ (min/nM) versus 1/[ATP] ($\mu M^{-1}$) at six fixed compound **6** concentrations [the b-FL-ATF2 concentration was fixed at 0.5 $\mu$M; the equation for competitive inhibition was fit to the experimental data (*31*)]; (B) double-reciprocal plot of $1/v$ (min/nM) versus 1/[b-FL-ATF2] ($\mu M^{-1}$) at six fixed compound **6** concentrations [the ATP concentration was fixed at 8 $\mu$M; the equation for pure noncompetitive inhibition was fit to the experimental data (*31*)].

the $K_m$ and $K_{ia}$ for either substrate, indicating discrete binding of the two substrate sites and suggesting the ability of either substrate to complex with the enzyme regardless of the occupancy of the second substrate site. The finding that $K_m$ and $K_{ia}$ are the same for both substrates in JNK3α1 is similar to that found by Niu et al. (*30*) and confirmed by our studies for JNK2α2, suggesting that both isoforms of JNK have non-interacting substrate sites. The random sequential mechanism suggested by the initial velocity studies was corroborated with the use of the dead-end ATP inhibitor, AMP−PCP, which showed the expected competitive inhibition pattern versus ATP and pure noncompetitive pattern versus b-FL-ATF2. We extended the inhibition analysis to include a putative ATF2 competitive peptide inhibitor (**1**) derived from the known δ-domain (*36*). Indeed, Barr et al. (*37*) had previously shown that an 11-mer peptide from the JNK-binding δ-domain spanning residues 46–56 of ATF2 had 31% inhibition of JNK1 at 1.7 $\mu$M. Our results were consistent with peptide **1** being competitive with b-FL-ATF2 and pure noncompetitive with ATP, further strengthening the interpretation that JNK3α1 proceeds via a random sequential ordered kinetic mechanism. This finding for JNK3α1 is fully consistent with the kinetic mechanism recently reported for JNK2α2, for which the authors demonstrated this same mechanism utilizing steady-state kinetic analysis and GST-ATF2 as substrate (*30*). It should also be noted that the $K_m$ values for both b-FL-ATF2 and ATP for JNK3α1 reported in our present study are nearly identical to those reported by Lisnock et al. (*11*) for JNK3α1 as well as those reported by Niu et al. (*30*) for JNK2α2.

Interestingly, the finding that both JNK3α1 and JNK2α2 (*30*) proceed by random sequential ordered mechanisms when ATF2 was utilized as the substrate is in contrast to the ordered sequential mechanism seen for p38 (*29*), a MAP kinase family member related to JNK. Similarly, the fact that $K_m$ and $K_{ia}$ for ATF2 and ATP are similar in magnitude when they are substrates for JNK3α1 and JNK2α2 (*30*), but have a nearly 12-fold difference in p38 (*29*), also speaks to the difference between these two MAP kinase family members. It should also be noted that p38 was shown to proceed by an ordered sequential kinetic mechanism with ATP binding first when a 21 amino acid peptide was used as the substrate (*34*), suggesting that phosphoryl acceptor affects the kinetic mechanism for p38. Furthermore, the $K_m$ for ATP when the 21 amino acid peptide was used as a substrate for p38 was 100 $\mu$M (*34*), 5-fold higher than the $K_m$ for ATP when GST-ATF2 was used as substrate for p38, suggesting that substrate affects ATP binding in p38. The increased $K_m$ for ATP on p38 was also seen when the EGRF peptide was used (*38*). In that study, Young et al. (*38*) found the $K_m$ for ATP = 200 $\mu$M, again suggesting that substrate affects ATP $K_m$for p38. Although these observations support the notion that JNK and p38 may have different kinetic mechanisms and different substrate interactions, it is unclear where the structural basis for this difference lies. One possible structural explanation comes from the recent paper by White et al., in which they have solved the crystal structure for the complex of murine p38 with its protein–substrate MAPKAP-2 (*39*). In that paper the authors show that there is a 1.7 Å rms deviation between the complexed structure and that of uncomplexed p38. They attributed this large rms deviation to a 5° rigid rotation movement of the N-lobe such that the ATP binding site becomes distorted upon substrate binding. It is interesting to speculate that rotation of the N-lobe in p38 requires the substrate to provide part of the ATP binding site and that substrate does not need to fulfill this role in JNK3 or JNK2.

*Mode of Inhibition for δ-Domain ATF2 Peptides.* The inability of peptides **4** and **5** to act as either substrates or inhibitors for JNK3α1 even at 1 mM concentration is consistent with previously reported biochemical results for the MAP kinase family member ERK2, for which binding studies utilizing Elk-1 showed that the phosphoacceptor site in Elk-1 is not essential for ERK-2 binding (*40*). Furthermore, our biochemical results for JNK3α1 also are consistent with the finding of Livingstone et al., who showed that δ-domain deletion mutants of ATF2, which contained intact phospho-acceptor sites, were not substrates for JNK in cell-based studies, implicating the necessity of the δ-domain region, but not the phosphoacceptor region, for binding (*20*). In contrast to the phosphoacceptor site peptides, the δ-domain peptide **1** was shown to be a competitive inhibitor versus b-FL-ATF2 and a pure noncompetitive inhibitor versus ATP. This result is consistent with the previous results of Barr et al. (*41*), who reported that the δ-domain peptide of ATF2 consisting of amino acids 46–56 had 31% inhibition of JNK1 at 1.7 $\mu$M. However, they did not report a mechanism of inhibition for this peptide, nor did they determine a $K_i$. Our results are therefore the first quantitative determination of the $K_i$ for this peptide (35.6 ± 1.9 $\mu$M; Table 2) and, equally importantly, the first demonstration that the δ-domain peptides can act as competitive inhibitors of ATF2 despite the fact that they lack the phosphoacceptor site.

*Mode of Inhibition for Compound* **6** Our kinetic data showed that compound **6** was an ATP competitive inhibitor and pure noncompetitive inhibitor versus b-FL-ATF2. The double-reciprocal plots of velocity versus concentration showed intersecting lines at the *y*-axis for compound **6** versus ATP, the paradigm for competitive inhibition. Correspondingly, double-reciprocal plots of compound **6** versus b-FL-ATF2 showed an intersection to the left of the *y*-axis, the model for noncompetitive inhibition. The minimal difference between the $K_{is}$ and $K_{ii}$ values indicated that compound **6** bound with equal affinity whether b-FL-ATF2 concentrations were $\ll K_m$ or approaching saturation. These findings are the first kinetic results to reveal this mode of inhibition for this class of compounds. The ATP competitive nature of compound **6** is consistent with that found for both anilinobipyridines and aminopyridines, two classes of related compounds having X-ray crystal structures revealing them to be bound in the ATP pocket (*42, 43*). Preliminary crystal structure data from our laboratory showed that compound **6** also bound in the ATP pocket (Habel et al., unpublished results).

*Mode of Inhibition for JIP Peptide.* The ATF2 δ-domain peptide (**1**) inhibited JNK3α1 via an ATF2 competitive mechanism, an expected outcome for an inhibitor designed to bind in the δ-domain docking groove of JNK. The JIP peptide inhibitor, **3**, also displayed a competitive binding mode versus b-FL-ATF2 for JNK3α1, which corresponded nicely to the data found by Niu et al. for this same peptide versus JNK2α2 (*30*). However, in our hands peptide **3** had a $K_i$ value 10-fold more potent for JNK2α2 (Supporting Information Table S2) than that found by Niu et al. (*30*) and 10-fold more potent for JNK1α1 based on the $IC_{50}$ (Supporting Information Table S3) than the binding studies of Heo et al. (*44*). In our work, the $IC_{50}$ values for peptide **3** versus JNK1α1, JNK2α2, and JNK3α1 were all within 4-fold, suggesting similar affinity for all three isoforms (Supporting Information Table S3). The results for JNK3α1 are the first presented and have no direct comparison in the literature. It is unclear why our $K_i$ values are approximately 10-fold more potent for JNK1α1 than the $K_d$ values found by Heo et al. (*44*), but it may be due to the differences in the methods used such as kinetic determination versus calorimetry utilized by Heo et al. (*44*).

The sequence for the docking groove on JNK1 to which peptide **3** binds has been revealed to include JNK1 residues 118−130, 159–163, and 324–329 via the solved X-ray complex (*44*). Alignment of these residues with the corresponding amino acids on JNK2 and JNK3 show complete identity for all residues within 4 Å of any corresponding JIP residue, consistent with our findings that the affinities for the interactions between JIP and the three JNK isozymes are comparable. MAPK kinases are known to have a single conserved docking groove that binds to activating kinases, transcription factors, substrate kinases, and inactivating phosphatases (*45, 46*). However, it remains unclear whether the conserved docking groove on JNK for the JIP peptide is the same groove utilized by MAPK kinases with the δ-sites of transcription factors ATF2 and c-jun as well as upstream kinases including MKK4 and MKK7 and MEK1 and MEK2 (*36, 45, 46*).

Recently, ter Haar et al. published the crystal structure of p38 complexed with its substrate, MAPKAP kinase 2 (MK2) (*47*). The structure clearly indicates that MK2 binds to the MAPK docking groove of p38. Although the p38 and JNK1 docking grooves for MK2 and JIP are not completely conserved, they are extremely similar. An overlay of the p38−MK2 complex (*39*) with the JNK1−JIP complex (*44*) suggests that the docking domain for MK2 in p38 is equivalent to the JIP docking domain in JNK1 (Figure 5). From this inference, it is rational to speculate that the conserved MAPK docking groove for δ-sites is the same region to which JIP binds to the JNK kinases. Chang et al. resolved the structure of p38 complexed with the peptides of a p38 activator, MKK3b, and a peptide from the transcription activator MEF2c (*48*). These peptides both bind in the MAPK docking groove, although they have little sequence homology to each other or to MK2. Although this supports the claim of a single nonspecific docking sequence, it also provides direct evidence that complexation of peptides with MAPK kinases mimic that of full-length proteins. Moreover, because our results indicated that JIP-1 peptide (**3**) is not an inhibitor of p38, despite some of the docking domain similarities, there are clearly differences in this domain among the MAPK kinase family members that allow for specificity between p38 and JNK.

FIGURE 5: Overlay of the JNK1 (green)−JIP (blue) complex (PDB ID: 1UKH) with the p38 (gray)−MK2 (yellow with magenta δ-site) complex (PDB ID: 2OKR) (rmsd = 1.85 Å), suggesting the δ-sites for JIP and MK2 bind to a conserved MAPK docking groove found in JNK1 and p38 (*39, 44*).

In summary, we have determined the kinetic mechanism for JNK3α1 to be random sequential for b-FL-ATF2 and ATP. Moreover, the $K_m$ and $K_{ia}$ values determined for these two substrates for JNK3α1 were very similar to those found for JNK2α2, suggesting similar binding affinities between these two isozymes. Furthermore, the similarity in affinity for the 11-mer JIP peptide (**3**) for the three JNK isozymes compared to the MAPK p38 suggests a potential avenue for the specific inhibition of JNK by JIP versus other MAP kinases, but selectivity within this domain among the JNK isoforms may be difficult. More detailed structural and site-directed mutagenesis studies will be needed to determine if isoform selectivity will be possible in the docking domain.

## ACKNOWLEDGMENT

We are grateful to Dr. Derek Duckett and Weimin Chen for generating some of the reagents used in this study. We thank Dr. Jeff Habel for generating the crystal structure

overlay. We are also grateful to Dr. Derek Duckett and Dr. Jeff Habel for their critical review of the manuscript.

## SUPPORTING INFORMATION AVAILABLE

Figures and a table of the $IC_{50}$ data for the three JNK isoforms with JIP-1 (**3**) as well as JNK3α1 with the short ATF2 peptide (**2**), a table of the inhibition constants for JNK2α2 versus JIP-1 (**3**), and a table for the kinetic constants of JNK3α1 using the full ternary equation. This material is available free of charge via the Internet at http://pubs.acs.org.

## REFERENCES


1. Roux, P. P., and Blenis, J. (2004) ERK and p38 MAPK-activated protein kinases: a family of protein kinases with diverse biological functions. *Microbiol. Mol. Biol. Rev. 68*, 320–344.
2. Gerits, N., Kostenko, S., and Moens, U. (2007) In vivo functions of mitogen-activated protein kinases: conclusions from knock-in and knock-out mice. *Transgenic Res. 16*, 281–314.
3. Ip, Y. T., and Davis, R. J. (1998) Signal transduction by the c-Jun N-terminal kinase (JNK)—from inflammation to development. *Curr. Opin. Cell Biol. 10*, 205–219.
4. Minden, A., and Karin, M. (1997) Regulation and function of the JNK subgroup of MAP kinases. *Biochim. Biophys. Acta: Rev. Cancer 1333*, F85–F104.
5. Yang, D. D., Kuan, C. Y., Whitmarsh, A. J., Rincon, M., Zheng, T. S., Davis, R. J., Rakic, P., and Flavell, R. A. (1997) Absence of excitotoxicity-induced apoptosis in the hippocampus of mice lacking the Jnk3 gene. *Nature 389*, 865–870.
6. Gupta, S., Barrett, T., Whitmarsh, A. J., Cavanagh, J., Sluss, H. K., Derijard, B., and Davis, R. J. (1996) Selective interaction of JNK protein kinase isoforms with transcription factors. *EMBO J. 15*, 2760–2770.
7. Zhang, Y., Zhou, L., and Miller, C. A. (1998) A splicing variant of a death domain protein that is regulated by a mitogen-activated kinase is a substrate for c-Jun N-terminal kinase in the human central nervous system. *Proc. Natl. Acad. Sci. U.S.A. 95*, 2586–2591.
8. Xie, X. L., Gu, Y., Fox, T., Coll, J. T., Fleming, M. A., Markland, W., Caron, P. R., Wilson, K. P., and Su, M. S. S. (1998) Crystal structure of JNK3: a kinase implicated in neuronal apoptosis. *Structure 6*, 983–991.
9. Martin, J. H., Mohit, A. A., and Miller, C. A. (1996) Developmental expression in the mouse nervous system of the p49(3F12) SAP kinase. *Mol. Brain Res. 35*, 47–57.
10. Mohit, A. A., Martin, J. H., and Miller, C. A. (1995) P49(3F12) Kinase—a novel MAP kinase expressed in a subset of neurons in the human nervous-system. *Neuron 14*, 67–78.
11. Lisnock, J., Griffin, P., Calaycay, J., Frantz, B., Parsons, J., O'Keefe, S. J., and LoGrasso, P. (2000) Activation of JNK3α1 requires both MKK4 and MKK7: Kinetic characterization of in vitro phosphorylated JNK3α1. *Biochemistry 39*, 3141–3148.
12. Hunot, S., Vila, M., Teismann, P., Davis, R. J., Hirsch, E. C., Przedborski, S., Rakic, P., and Flavell, R. A. (2004) JNK-mediated induction of cyclooxygenase 2 is required for neurodegeneration in a mouse model of Parkinson's disease. *Proc. Natl. Acad. Sci. U.S.A. 101*, 665–670.
13. Morishima, Y., Gotoh, Y., Zieg, J., Barrett, T., Takano, H., Flavell, R., Davis, R. J., Shirasaki, Y., and Greenberg, M. E. (2001) β-Amyloid induces neuronal apoptosis via a mechanism that involves the c-Jun N-terminal kinase pathway and the induction of Fas ligand. *J. Neurosci. 21*, 7551–7560.
14. Cohen, P. (2002) The origins of protein phosphorylation. *Nat. Cell Biol. 4*, E127–E130.
15. Biondi, R. M., and Nebreda, A. R. (2003) Signalling specificity of Ser/Thr protein kinases through docking-site-mediated interactions. *Biochem. J. 372*, 1–13.
16. Seidel, J. J., and Graves, B. J. (2002) An ERK2 docking site in the Pointed domain distinguishes a subset of ETS transcription factors. *Genes Dev. 16*, 127–137.
17. Sharrocks, A. D., Yang, S. H., and Galanis, A. (2000) Docking domains and substrate-specificity determination for MAP kinases. *Trends Biochem. Sci. 25*, 448–453.
18. Tanoue, T., and Nishida, E. (2002) Docking interactions in the mitogen-activated protein kinase cascades. *Pharmacol. Ther. 93*, 193–202.
19. Gupta, S., Campbell, D., Derijard, B., and Davis, R. J. (1995) Transcription factor ATF2 regulation by the JNK signal-transduction pathway. *Science 267*, 389–393.
20. Livingstone, C., Patel, G., and Jones, N. (1995) ATF-2 contains a phosphorylation-dependent transcriptional activation domain. *EMBO J. 14*, 1785–1797.
21. Yang, S. H., Whitmarsh, A. J., Davis, R. J., and Sharrocks, A. D. (1998) Differential targeting of MAP kinases to the ETS-domain transcription factor Elk-1. *EMBO J. 17*, 1740–1749.
22. Kallunki, T., Deng, T. L., Hibi, M., and Karin, M. (1996) c-jun Can recruit JNK to phosphorylate dimerization partners via specific docking interactions. *Cell 87*, 929–939.
23. Ito, M., Yoshioka, K., Akechi, M., Yamashita, S., Takamatsu, N., Sugiyama, K., Hibi, M., Nakabeppu, Y., Shiba, T., and Yamamoto, K. (1999) JSAP1, a novel Jun N-terminal protein kinase (JNK)-binding protein that functions as a scaffold factor in the JNK signaling pathway. *Mol. Cell. Biol. 19*, 7539–7548.
24. Whitmarsh, A. J., Cavanagh, L., Tournier, C., Yasuda, L., and Davis, R. J. (1998) Mammalian scaffold complex that selectively mediates MAP kinase activation. *Science 281*, 1671–1674.
25. Yasuda, J., Whitmarsh, A. J., Cavanagh, J., Sharma, M., and Davis, R. J. (1999) The JIP group of mitogen-activated protein kinase scaffold proteins. *Mol. Cell. Biol. 19*, 7245–7254.
26. Cook, P. F., Neville, M. E., Vrana, K. E., Hartl, F. T., and Roskoski, R. (1982) Adenosine cyclic 3′, 5′-monophosphate dependent protein-kinase—kinetic mechanism for the bovine skeletal-muscle catalytic subunit. *Biochemistry 21*, 5794–5799.
27. Whitehouse, S., Feramisco, J. R., Casnellie, J. E., Krebs, E. G., and Walsh, D. A. (1983) Studies on the kinetic mechanism of the catalytic subunit of the cAMP-dependent protein-kinase. *J. Biol. Chem. 258*, 3693–3701.
28. Whitehouse, S., and Walsh, D. A. (1983) Mg.ATP2-dependent interaction of the inhibitor protein of the cAMP-dependent protein-kinase with the catalytic subunit. *J. Biol. Chem. 258*, 3682–3692.
29. LoGrasso, P. V., Frantz, B., Rolando, A. M., Okeefe, S. J., Hermes, J. D., and Oneill, E. A. (1997) Kinetic mechanism for p38 MAP kinase. *Biochemistry 36*, 10422–10427.
30. Niu, L. H., Chang, K. C., Wilson, S., Tran, P., Zuo, F. R., and Swinney, D. C. (2007) Kinetic characterization of human JNK2α2 reaction mechanism using substrate competitive inhibitors. *Biochemistry 46*, 4775–4784.
31. Leatherbarrow, R. J. (1998) GraFit, 5 ed., Erithacucs Software Ltd., Staines, U.K.
32. Kois, A., MacFarlane, K., Satoh, Y., Bhagwat, S., Shripad, S., Parnes, J., Palanki, M., and Erdman, P. (2004) Preparation of anilinopyramidines as JNK pathway inhibitors, United States of America, Patent WO 2002046170.
33. Cleland, W. W. (1963) Kinetics of enzyme-catalyzed reactions with 2 or more substrates or products. 3. Prediction of initial velocity and inhibition patterns by inspection. *Biochim. Biophys. Acta 67*, 188.
34. Chen, G. J., Porter, M. D., Bristol, J. R., Fitzgibbon, M. J., and Pazhanisamy, S. (2000) Kinetic mechanism of the p38-alpha MAP kinase: Phosphoryl transfer to synthetic peptides. *Biochemistry 39*, 2079–2087.
35. Segel, I. H. (1975) *Enzyme Kinetics*, Wiley, New York.
36. Ho, D. T., Bardwell, A. J., Abdollahi, M., and Bardwell, L. (2003) A docking site in MKK4 mediates high affinity binding to JNK MAPKs and competes with similar docking sites in JNK substrates. *J. Biol. Chem. 278*, 32662–32672.
37. Barr, R. K., Kendrick, T. S., and Bogoyevitch, M. A. (2002) Identification of the critical features of a small peptide inhibitor of JNK activity. *J. Biol. Chem. 277*, 10987–10997.
38. Young, P. R., McLaughlin, M. M., Kumar, S., Kassis, S., Doyle, M. L., McNulty, D., Gallagher, T. F., Fisher, S., McDonnell, P. C., Carr, S. A., Huddleston, M. J., Seibel, G., Porter, T. G., Livi, G. P., Adams, J. L., and Lee, J. C. (1997) Pyridinyl imidazole inhibitors of p38 mitogen-activated protein kinase bind in the ATP site. *J. Biol. Chem. 272*, 12116–12121.
39. White, A., Pargellis, C. A., Studts, J. M., Werneburg, B. G., and Farmer, B. T. (2007) Molecular basis of MAPK-activated protein kinase 2: p38 assembly. *Proc. Natl. Acad. Sci. U.S.A. 104*, 6353–6358.
40. Yang, S. H., Yates, P. R., Whitmarsh, A. J., Davis, R. J., and Sharrocks, A. D. (1998) The Elk-1 ETS-domain transcription factor contains a mitogen-activated protein kinase targeting motif. *Mol. Cell. Biol. 18*, 710–720.
41. Barr, R. K., Boehm, I., Attwood, P. V., Watt, P. M., and Bogoyevitch, M. A. (2004) The critical features and the mechanism

of inhibition of a kinase interaction motif-based peptide inhibitor of JNK. *J. Biol. Chem. 279*, 36327–36338.

42. Swahn, B. M., Xue, Y. F., Arzel, E., Kallin, E., Magnus, A., Plobeck, N., and Viklund, J. (2006) Design and synthesis of 2′-anilino-4,4′-bipyridines as selective inhibitors of e-Jun N-terminal kinase-3. *Bioorg. Med. Chem. Lett. 16*, 1397–1401.
43. Alam, M., Beevers, R. E., Ceska, T., Davenport, R. J., Dickson, K. M., Fortunato, M., Gowers, L., Haughan, A. F., James, L. A., Jones, M. W., Kinsella, N., Lowe, C., Meissner, J. W. G., Nicolas, A.-L., Perry, B. G., Phillips, D. J., Pitt, W. R., Platt, A., Ratcliffe, A. J., Sharpe, A., and Tait, L. J. (2007) Synthesis and SAR of aminopyrimidines as novel c-Jun N-terminal kinase (JNK) inhibitors. *Bioorg. Med. Chem. Lett. 17*, 3463–3467.
44. Heo, J. S., Kim, S. K., Seo, C. I., Kim, Y. K., Sung, B. J., Lee, H. S., Lee, J. I., Park, S. Y., Kim, J. H., Hwang, K. Y., Hyun, Y. L., Jeon, Y. H., Ro, S., Cho, J. M., Lee, T. G., and Yang, C. H. (2004) Structural basis for the selective inhibition of JNK1 by the scaffolding protein JIP1 and SP600125. *EMBO J. 23*, 2185–2195.
45. Bardwell, L. (2006) Mechanisms of MAPK signalling specificity. *Inf. Process. Mol. Signalling* 837–841.
46. Bardwell, A. J., Abdollahi, M., and Bardwell, L. (2003) Docking sites on mitogen-activated protein kinase (MAPK) kinases, MAR phosphatases and the Elk-1 transcription factor compete for MAPK binding and are crucial for enzymic activity. *Biochem. J. 370*, 1077–1085.
47. ter Haar, E., Prabakhar, P., Liu, X., and Lepre, C. (2007) Crystal structure of the P38 α-MAPKAP kinase 2 heterodimer. *J. Biol. Chem. 282*, 9733–9739.
48. Chang, C. I., Xu, B. E., Akella, R., Cobb, M. H., and Goldsmith, E. J. (2002) Crystal structures of MAP kinase p38 complexed to the docking sites on its nuclear substrate MEF2A and activator MKK3b. *Mol. Cell 9*, 1241–1249.

BI701852Z